Soft Matter

www.softmatter.org

Volume 6 | Number 22 | 21 November 2010 | Pages 5647–5818

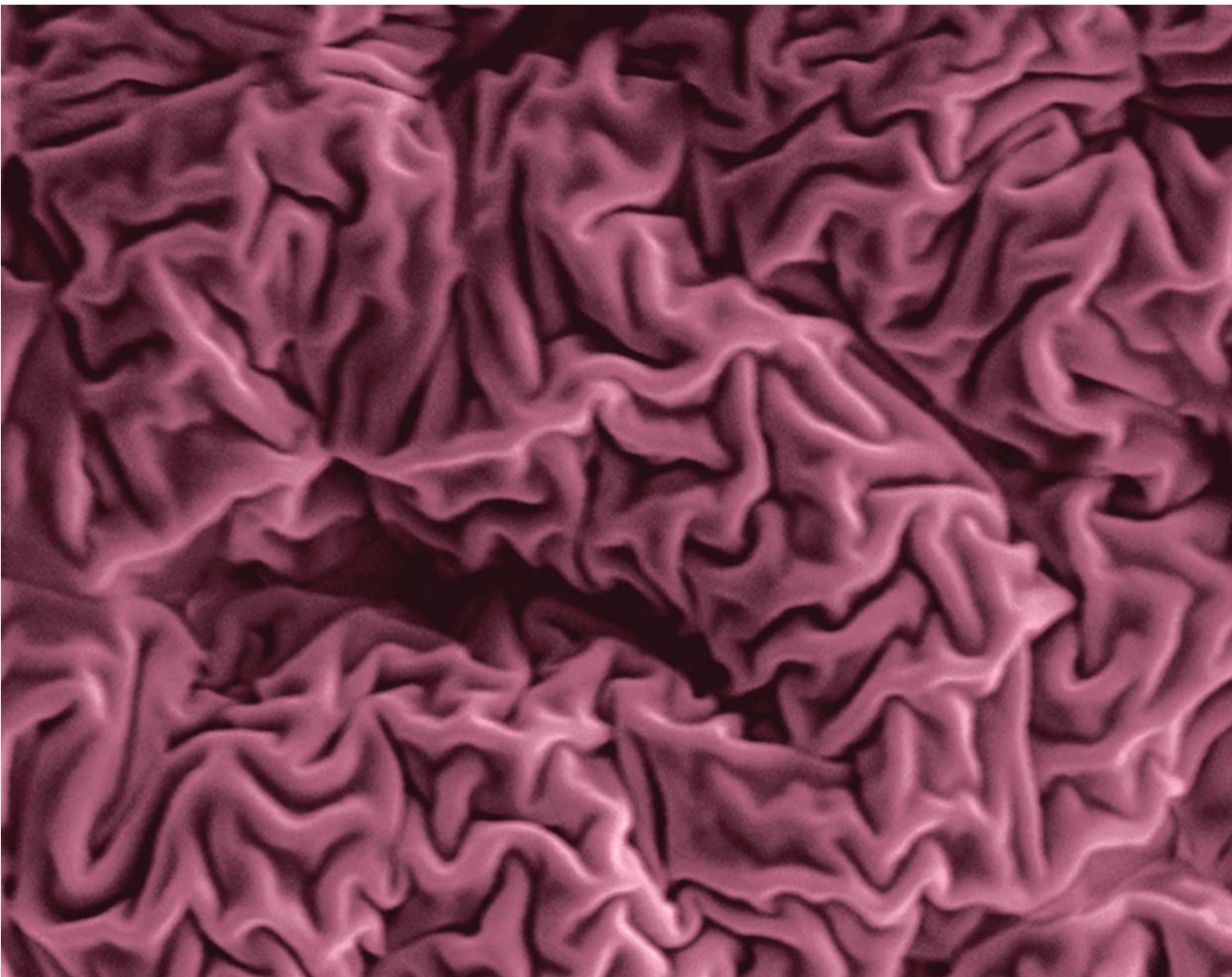

Themed issue: The Physics of Buckling

ISSN 1744-683X

RSC Publishing

PAPER

Ashkan Vaziri *et al.*

High aspect ratio wrinkles on a soft polymer

1744-683X(2010)6:22;1-O

High aspect ratio wrinkles on a soft polymer†

Sk. Faruque Ahmed,[a] Geon-Ho Rho,[a] Kwang-Ryeol Lee,[a] Ashkan Vaziri*[b] and Myoung-Woon Moon*[a]

Received 16th May 2010, Accepted 20th July 2010
DOI: 10.1039/c0sm00386g

Instability of a stiff thin film attached to a compliant substrate often leads to the emergence of exquisite wrinkles with length scales that depend on the system geometry and applied stresses. These patterns have vast potential applications including in tissue engineering, flexible electronics and the semiconductor industry. However, one of the limiting factors in the usage of these patterns is the low amplitude/wavelength ratio that can be achieved using the current surface engineering techniques. Here, we present an effective method that allows the creation of wrinkles with an amplitude/wavelength aspect ratio as large as 2.5 on a soft polymer. In this method, first, the surface of a poly(dimethylsiloxane) (PDMS) is pre-patterned using an Ar ion beam. Then, an amorphous carbon film gets deposited on the pre-patterned polymeric surface using glancing angle deposition (GLAD). We show that the amplitude of the created patterns can be varied between several nm to submicron size by changing the carbon deposition time, allowing us to harness patterned polymeric substrates for a variety of applications. Specifically, we demonstrate a potential application of the high aspect ratio wrinkles for changing the surface optical band gap.

Introduction

Cracking, buckling, wrinkling, and in general mechanical instabilities, in thin films are generally treated as a nuisance.[1–4] This view has changed recently with the development of robust techniques for controlled patterning of polymer and hard surfaces and the emergence of novel applications that benefit from the created patterns.[5–8] These applications range from building cell templates and nanochannels for protein condensation to manufacturing smart adhesives and optical grating devices.[9–12]

A common class of these techniques is based on inducing a strain mismatch between a stiff thin film and a soft substrate, causing the instability and wrinkling of the stiff film. The wrinkle wavelength is determined by the system geometry (mainly the film thickness) and the relative stiffness of the film and substrate,[8,13,14] and is in general much larger than the film thickness and much smaller than the specimen dimensions. The amplitude of the wrinkles depends on the applied stresses and the magnitude of the induced strain mismatch.[15–17] The ratio of wrinkle amplitude/wavelength is normally limited to 1/10.

In this study, we created buckle patterns with high amplitude/wavelength ratio by the deposition of an amorphous carbon film on a surface of a soft polymer poly(dimethylsiloxane) (PDMS). We employed glancing angle deposition (GLAD) for deposition of an amorphous carbon film on a PDMS surface. Amorphous carbon films are used as a protective layer in structural systems and biomedical components, due to their low friction coefficient, wear resistance, and high elastic modulus and hardness.[18,19] The deposited carbon layer is generally under high residual compressive stresses (~1 GPa), making it susceptible to buckle delamination on a hard substrate (*e.g.* silicon or glass)[3,20,21] and to wrinkling on a soft substrate.[22] GLAD is a physical vapour deposition method used to fabricate functional thin films with a columnar morphology. The application of the created morphologies range from sensors and actuators to optical filters, microfluidics, and catalysis.[23–27]

Fig. 1a shows the schematic of a PDMS substrate subjected to hydrocarbon ion beam irradiation, and the scanning electron microscopy (SEM) images of wrinkles created by 50 min amorphous carbon film deposition at three different incident angles. The deposited carbon film is under approximately equi-biaxial compressive stress,[3,21] and the created wrinkles are semi-herringbone or semi-labyrinth shapes, Fig. 1b–1d. The wavelength of the

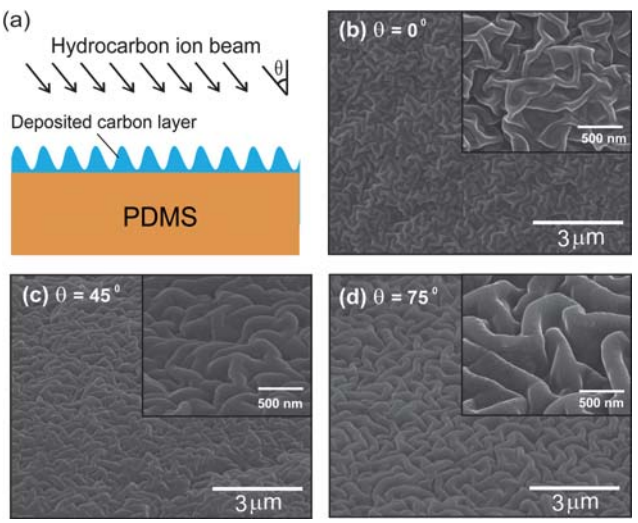

Fig. 1 Surface patterns created by carbon film deposition. (a) Schematic of the experiments, (b–d) SEM images of the PDMS surface after 50 min carbon film deposition at different incident angles.

[a]*Interdisciplinary and Fusion Technology Division, Korea Institute of Science and Technology, 136-791 Seoul, Republic of Korea*
[b]*Department of Mechanical and Industrial Engineering, Northeastern University, Boston, MA, 02115, USA. E-mail: vaziri@coe.neu.edu; mwmoon@kist.re.kr*

† This paper is part of a *Soft Matter* themed issue on The Physics of Buckling. Guest editor: Alfred Crosby.

wrinkles is relatively insensitive to the deposition angle and duration and is $\sim$ 750 nm. In contrast, the amplitude of the wrinkles depends on the deposition angle and duration. The wrinkles created by 50 min carbon deposition normal to the substrate surface (*i.e.* $\theta = 0°$, Fig. 1b) has an average amplitude 144 nm (*i.e.* amplitude/wavelength $\sim$ 1/5) and has the appearance of nonlinear wrinkle configurations observed in a biaxially-compressed film on a compliant substrate.[16,22] The patterns formed by deposition at 45° and 75° have approximately the same wavelength, but much higher amplitudes (amplitude/wavelength ratios of $\sim$ 2 and 2.5, respectively). Fig. 2a–2c displays the SEM images of surface patterns created by carbon film deposition at 75° with different deposition durations, showing that the wrinkle amplitude increases for longer deposition durations. Ion or plasma treatment at an oblique angle results in formation of a porous thin film with anisotropic features that are induced by the atomic-scale shadowing, or self-shadowing.[24,27] As the ion or radical nucleates on the target substrate, the deposition rate is higher in front of the nucleus than the deposition rate behind it, due to the shadowing by the nucleus, resulting in a porous film structure.[24] At early stages of the deposition, wrinkles could emerge due to the relaxation of the strain energy in a compressively stressed thin film as shown in Fig. 2a. For a longer deposition time, the porous structure keeps growing on the wrinkled surface, resulting in an increase in the surface amplitude as shown in Fig. 2b and 2c. In Fig. 2d, we measured the amplitude/wavelength ratio of patterns created on a PDMS surface at three different deposition incident angles as a function of the deposition time. At an incident angle 0° and 45°, the amplitude/wavelength ratio is relatively independent of the deposition time (in the range studied here, 30 s–50 min) and is 1/10 and 1/2, respectively. In contrast, the amplitude/wavelength ratio of the patterns created with the incident angle 75°, increases by increasing the deposition duration, resulting to an amplitude/wavelength ratio aspect ratio as high as 2.5.

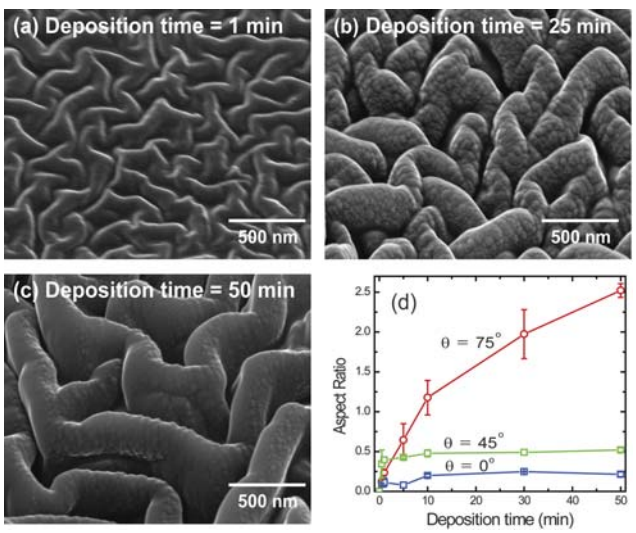

Fig. 2 The effect of deposition angle and time on the morphology. (a–c) SEM images of the PDMS surface after carbon film deposition at 75° incident angles for three different deposition durations. (d) Aspect ratio of the amplitude to wavelength for patterns created by carbon film deposition at different angles, *versus* the deposition time.

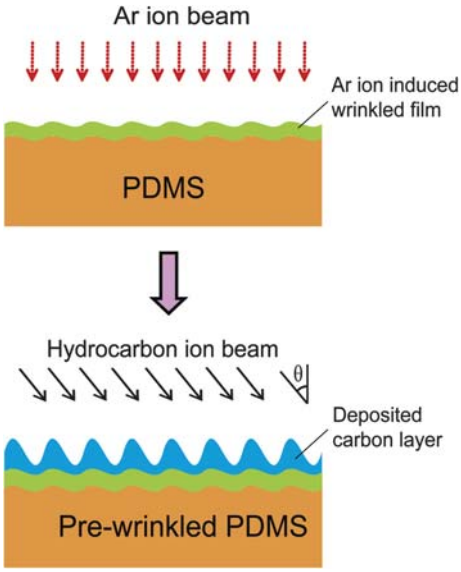

Fig. 3 Schematic of the fabrication of pre-wrinkle patterns on PDMS by Ar ion beam (top) and subsequent carbon deposition using GLAD to increase the amplitude of the pre-patterned surface (bottom).

As an extension of this technique, we demonstrated that the amorphous carbon deposition on a pre-patterned polymeric surface allows fabrication of high aspect ratio wrinkles. Fig. 3 shows the schematic of our experiments; first, we pre-patterned the surface of PDMS by Ar ion beam irradiation. The created patterns are in the form of two-dimensional wrinkles with a wavelength that depends on the treatment time and was varied between 200 to 1400 nm in this study. In the next step, an amorphous carbon film gets deposited on the pre-patterned surface using GLAD to elevate the amplitude of the patterns. The details of the proposed method are outlined in the following section. As a part of our discussion, we will demonstrate an interesting application of the created high aspect ratio wrinkles for controlling the optical band gap with respect to the wavelength of wrinkles.

Experimental methods

Wrinkle patterns with a high amplitude/wavelength ratio were fabricated with irradiation of Ar ion beam on a PDMS substrate and a subsequent deposition of an amorphous carbon film using GLAD. PDMS substrates were prepared by a mixture of elastomer and cross-linker in a mass ratio of 10 : 1 (Sylgard-184, Dow Corning, MI, USA). The mixture was placed in a plastic box and stirred to remove trapped air bubbles and then, cured at 80 °C for 2 h, resulting in a cross-linked PDMS network, which was cut as coupons of 20mm × 20mm × 3mm for the experiments.

The Ar ion beam treatment of PDMS and also the carbon film deposition were carried out in a linear ion gun (DC 3 kV/6 kW, EN Technologies).[28] The sample coupons were placed in the ion beam chamber, and the chamber was evacuated to a base pressure 2×10^{-5} mbar. The distance between the ion source and the substrate holder was approximately 15 cm. Ar gas was introduced into the end-hall type ion gun to obtain Ar ions with a flow rate of 8 standard cubic centimeters per minute (sccm). The

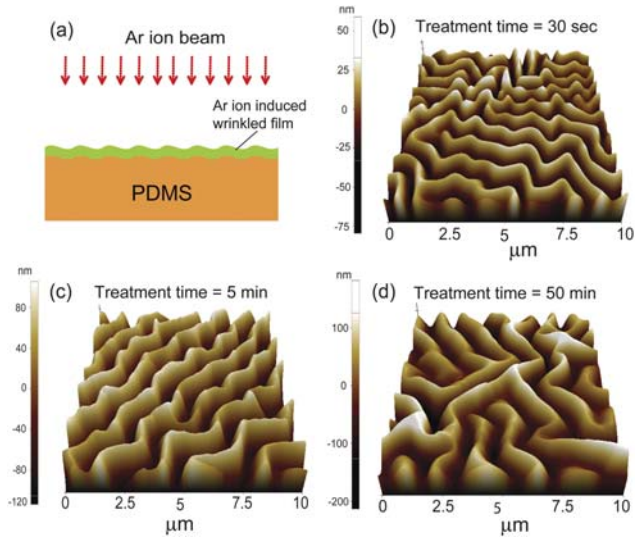

Fig. 4 Ar ion treatment of PDMS. (a) Schematic of the experiment. (b–d) AFM images of the wrinkles formed by the ion beam irradiation with different treatment times on the surface of PDMS.

anode voltage was kept at a constant value of 1 kV with a current density 50 μA/cm^2. A radio frequency (r.f.) bias voltage was applied to the substrate holder at a bias voltage of −600 V and a corresponding current of 44 mA. The PDMS was exposed to Ar ion beam for 10 s to 50 min, leading to creation of wrinkles. The amorphous carbon film was deposited on flat, as well as pre-patterned PDMS coupons by introducing the acetylene (C_2H_2) into the ion gun at a flow rate of 8 sccm. During carbon deposition, the anode voltage was kept at a constant value of 1 kV and a radio frequency (r.f.) bias voltage was applied to the substrate holder at a bias voltage of −200 V. In this study, the carbon deposition time was kept between 30 s to 50 min, while the incident angle of hydrocarbon ion was varied from 0° to 75°.

The morphology of the created patterns was measured with an atomic force microscope (AFM, XE-100, Park Systems) and a scanning electron microscope (SEM, NanoSEM, FEI Company). In each experiment, the morphology of the surface patterns was measured on five different surface regions of the polymer. Raman spectroscopy analyses were performed on wrinkled amorphous carbon surfaces to investigate the ion-induced chemical changes of the surface layer. The Raman measurements were made in a backscattering geometry with a Raman spectrometer (LabRAM HR, HORIBA Jobin-Yvon Inc.) filled with a liquid-nitrogen cooled CCD detector. The spectra were collected for 120 s under ambient conditions using a 514.5 nm line of argon-ion laser with a power of 0.5 mW. The UV-Vis measurements were performed in the wavelength range of 200–800 nm using a spectrophotometer (Cary 5000 UV-Vis-NIR spectrophotometer) at room temperature. The spectra were recorded by taking a PDMS sample as reference, thus, the transmission only due to the Ar treated surface layer and amorphous carbon film was measured.

Result and discussion

Fig. 4 shows AFM profile images of three different wrinkle patterns created on a PDMS surface by Ar ion beam irradiation. Ion beam irradiation results into the formation of a thin stiff skin on the polymer surface which is ∼ 100 times stiffer than PDMS and is under compressive stress.[29,30] The morphology of the created patterns depends on the state of stress in the thin film. For the ion beam irradiation normal to the polymeric surface, the state of stress in the thin film is semi-equal biaxial and the wrinkles are semi-labyrinth shape. The wrinkle wavelength mainly depends on the film thickness, t, and the ratio of elastic moduli of thin film and substrate, E_f/E_s and can be estimated from, $\lambda = \alpha t(E_f/E_s)^{1/3}$, where α is a constant (*e.g.* $\alpha = 4.36$ for the plane strain condition).[8,13,14] In Fig. 5b, we have plotted the wrinkle wavelength *versus* the Ar treatment time, which was

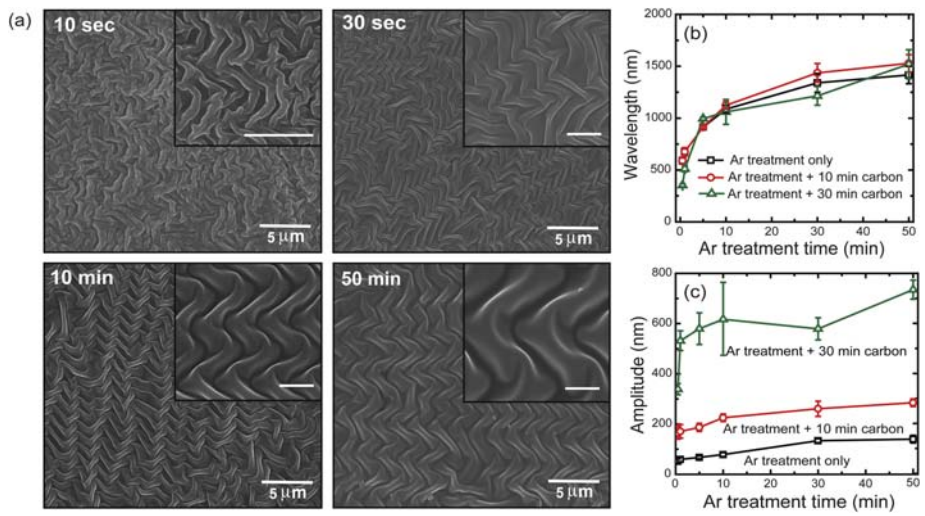

Fig. 5 (a) SEM images of the PDMS surface, pre-patterned by Ar ion with different treatment times (10 s–50 min) and then subjected to 10 min carbon film deposition at 75° incident angles. The scale bars in the insets are 1 μm. Dependence of the wavelength (b) and amplitude (c) of created patterns on the Ar ion treatment time. The carbon deposition incident angle was 75°.

varied between 30 s and 50 min. The created patterns have a wavelength in the range of 300 nm to 1500 nm. The amplitude of a created wrinkle, A, can be estimated from, $A \cong t(\varepsilon_0/\varepsilon_c - 1)^{1/2}$, where ε_0 is the applied strain and ε_c is the critical strain associated with the onset of instability. The amount of applied strain is limited by the nature of the polymer (*e.g.* PDMS generally ruptures when the applied strain is $\sim 100\%$). Thus, the amplitude of the created patterns is generally on the order of the film thickness (*e.g.* for PDMS subjected to ion beam irradiation, $\varepsilon_c \approx 3\%$,[15,29] which gives and upper limit of approximately $6 \times t$ for the wrinkle wavelength, where t is the film thickness). The thickness of the thin film is limited by the ion penetration and is generally in the range of 10–100 nm. Fig. 5b displays the dependence of the wrinkle amplitude on the Ar ion treatment time. The amplitude/wavelength ratio is always smaller than 1/10, although the wavelength changes by varying the treatment time quite considerably – see Fig. 5b. As shown in Figs. 1 and 2, the deposition of an amorphous carbon film on a polymeric surface results in the formation of herringbone-type wrinkle patterns, with an amplitude that depends on the deposition angle and duration. The wavelength of the patterns formed by carbon deposition on a flat PDMS surface is relatively insensitive to the deposition angle and duration. To select the wavelength of the patterns, we have deposited a carbon film on a polymeric surface pre-patterned by Ar ion beam irradiation. Fig. 5a shows SEM images of four different patterns created on pre-patterned PDMS surfaces. The amorphous carbon deposition angle and duration were 75° and 10 min, respectively, while the duration of Ar ion beam irradiation in the pre-patterning step was varied between 10 s and 50 min. Fig. 5b and 5c shows the measured wavelength and amplitude of patterns after 10 min and 30 min carbon deposition on a pre-patterned polymeric surface. The amorphous carbon deposition does not change the wavelength of a pre-patterned surface considerably, while elevating the surface amplitude. For 10 min carbon deposition, the thickness of the deposited carbon film is ~100–150 nm in all cases, leading to an amplitude/wavelength ratio in the range of 1/5 to 1/2.5 (note that a higher ratio is achieved for a pattern with a smaller wavelength). For 30 min carbon deposition, the carbon layer thickness is approximately 500–600 nm, leading to an amplitude/wavelength ratio as large as 1.

Characterization of the amorphous carbon film

Fig. 6a shows the Raman spectra of a pristine PDMS, a PDMS treated by Ar ion treated for 10 min and a PDMS after amorphous carbon films deposition at 0° and 75° incident angles and with different durations. There is no significant change in Raman spectra of an Ar treated PDMS compared to a pristine PDMS. The Raman spectrum of a deposited carbon film was deconvoluted using Gaussian distribution. A linear background into two peaks located at 1365 cm^{-1} and 1535 cm^{-1} represent disordered graphite clusters with short range of crystallinity (denoted as D peak) and graphite-like sp^2 bonded carbon (denoted as G peak), respectively.[31] In the Raman spectra, the G peak position shifts to a higher wave number for a longer amorphous carbon deposition time and also as the deposition angle is changed from 75° to 0°. This change indicates an increase in the sp^2 bonded aromatic sites. The graphitization of the films is also observed as the intensity of the D peak increases and the shoulder is more pronounced. Fig. 6b shows that the intensity ratio of the D peak to the G peak (I_D/I_G) increases by increasing the deposition time and by decreasing the deposition angle. This suggests that the number and/or size of sp^2 graphite clusters increases and the amorphous carbon film becomes more graphitic. The stress in the amorphous carbon film is known to decrease with increasing the sp^2 content. So with increasing the anode voltage, the sp^2 fraction increases and the stress in the amorphous carbon film decreases. The hardness of the film is associated with the full width and half maximum (FWHM) of G peak (with decreasing the FWHM of the G peak, the hardness of the amorphous carbon films decreases).[32] Fig. 6b shows that the FWHM of an amorphous carbon film is approximately independent of the deposition time and incident angle, thus, the hardness of the carbon film might be relatively insensitive to these parameters. Based on the Raman analysis, the newly-formed amorphous carbon film deposited using GLAD is almost identical to a carbon film deposited at a normal incident angle.[33,34]

Optical band gap characterization

PDMS is highly transparent in UV to near infrared regions. Commercially available PDMS contain silica nanoparticles, which reduce the unwanted scattering of light. Due to these unique properties, PDMS is used in various optical devices, including microlenses, waveguide components and optical

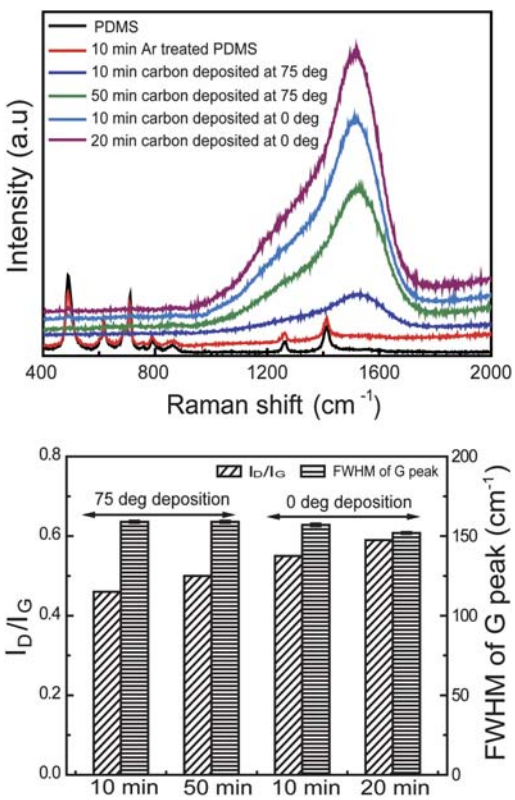

Fig. 6 (a) Raman spectra of PDMS, Ar ion treated PDMS and PDMS with amorphous carbon films deposition at different deposition angles and durations. (b) The corresponding I_D/I_G and FWHM of G peak profile.

grating.[35–38] Cai *et al.* fabricated the multimode waveguide with a low optical insertion loss and a high thermal stability using PDMS.[36] Bowden *et al.* fabricated a wrinkle-based diffraction grating.[38] The angular displacement of the first order diffraction spot on the grating was found to be linearly proportional to the strain applied on the PDMS before a plasma oxidation.[38] A very detailed study of wrinkle applications in optical grating technology has been reported by Harrison and coworkers.[11] They have reported that the intensity of the diffraction peaks in small angle light scattering experiments can change over three orders of magnitude by varying the strain imposed to the specimen by only 10%.

In the current study, we have tuned the optical band gap of a PDMS surface using the patterning method described in the previous section. The optical transmittance spectra of the Ar ion treated PDMS before and after amorphous carbon deposition are plotted in Fig. 7a, showing a gradual decrease in the transparency, as well as a shift from near UV to the 'visible region', by increasing the Ar ion treatment time. According to the band theory of solids, the absorption coefficient, α, can be calculated from $I(t) = I_o e^{-\alpha t}$, where I_o and $I(t)$are the intensities of the incident and transmitted light, respectively, and t is the film thickness. Using the transmittance data, the optical band gap energy, E_g, of a patterned PDMS surface can be obtained from Tauc expression,[39] $\alpha\, h\nu = A_f(h\nu - E_g)^n$, where $h\nu$ is the incident photon energy and A_f is a constant that arises from the Fermi's golden rule for fundamental band to band electronic transitions within the framework of a parabolic approximation for the dispersion relation.[40] $h\nu$ is the incident photon energy and the exponent n depends on the transition type. Here, $n = 1/2$, since direct transition is allowed to occur vertically from the top of the valence band to the bottom of the conduction band, while non-vertical transitions are normally forbidden.[42] To determine the possible transitions, we plotted $(\alpha h\nu)^{1/n} = (\alpha h\nu)^2$ *versus* the photon energy ($h\nu$) in Figs. 7b and 7c for an Ar ion treated PDMS surface and a pre-patterned PDMS surface with carbon film deposition, respectively. A linear relationship and the corresponding band gaps were obtained from extrapolating the straight section of the graph to, evaluate the value of $h\nu$ at at $\alpha = 0$, as shown by the dashed lines in Fig. 7b and 7c.[41]

Fig. 7d shows that the optical band gap of an Ar ion treated PDMS surface decreases from 3.57 to 3.33 eV by changing the ion treatment time in the range of 10–50 min. A longer Ar ion treatment results in the formation of a thicker surface layer and inherently, a higher level of defect and a stronger optical absorption in the sample.[43,44] The deposition of a carbon film for

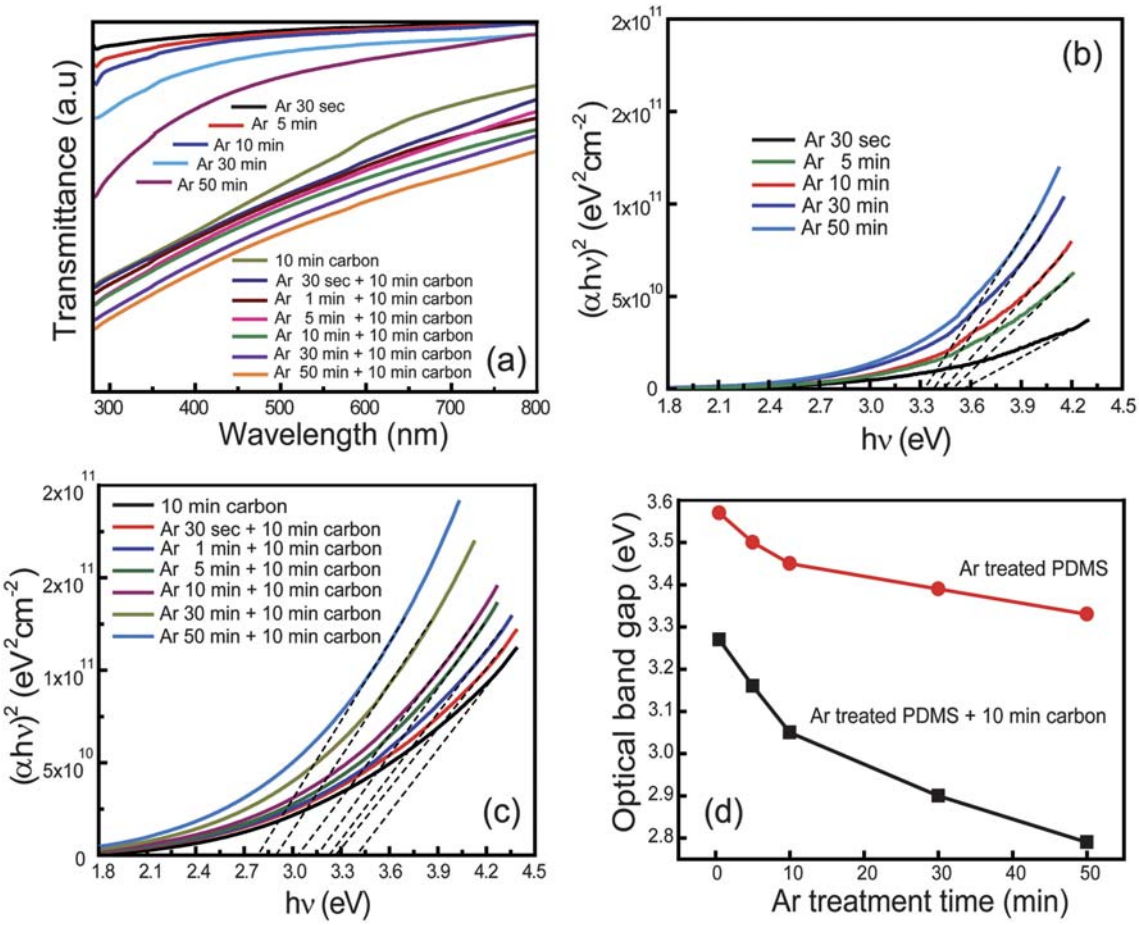

Fig. 7 (a) Transmittance spectra of the Ar ion treated PDMS and amorphous carbon deposited on Ar ion treated PDMS. (b–c) Tauc plot to determine the optical band gap for Ar ion treated PDMS and for high aspect ratio wrinkles made by amorphous carbon film deposition on pre-patterned surfaces. (d) Variation of optical band gap with Ar ion treatment time.

10 min results in a reduction in the optical band gap from 3.27 to 2.79 eV. The optical properties of an amorphous carbon film can be changed by changing the chemical bonding structure and by doping of different elements. For example, the optical band gap was shown to decrease from 2.55 to 1.95 eV by 12.5% Ag doping in DLC.[41] Surface wrinkling can also change the optical band gap.[45,46] However, the change in the optical gap achieved in this study based on high aspect ratio wrinkle patterns is considerably more significant. The reduction on the high aspect ratio wrinkle could be attributed to the presence of defects, which increases the density of localized states and consequently decreases the energy gap.[41] Moreover, the optical properties are likely to be controlled by nanoscale surface features created by the Ar ion beam irradiation and carbon deposition. The wrinkle wavelength increases for a longer Ar ion treatment time, resulting in a reduction in the optical band gap.

Summary

We presented a fabrication method of wrinkles with high aspect ratio of amplitude over wavelength using a glancing angle deposition (GLAD). First, we created wrinkles on a PDMS surface using Ar ion beam irradiation. The wrinkles had a wavelength in the range of 200–1400 nm depending on the ion treatment time. Then, an amorphous carbon film was deposited on the pre-patterned PDMS to elevate the amplitude of surface features. An application of polymeric surfaces, decorated with high aspect ratio wrinkles, was demonstrated for changing the optical band gap, which could have potential use in fabrication of optical devices.

Acknowledgements

This work was supported in part by grant 2E21580 from KIST project (KRL), and by CNMT under 21st Century Frontier R&D Programs from MEST (2010K000298) and in part by the U.S. Air Force Office of Scientific Research under AFOSR YIP grant award, grant # FA9550-10-1-0145 (AV). The authors declare no conflict of interest.

References

1 C. M. Stafford, C. Harrison, K. L. Beers, A. Karim, E. J. Amis, M. R. Vanlandingham, H. Kim, W. Volksen, R. D. Miller and E. E. Simonyi, *Nat. Mater.*, 2004, **3**, 545–550.
2 K. Efimenko, M. Rackaitis, W. Manias, A. Vaziri, L. Mahadevan and J. Genzer, *Nat. Mater.*, 2005, **4**, 293–297.
3 M.-W. Moon, H. M. Jensen, J. W. Hutchinson, K. H. Oh and A. G. Evans, *J. Mech. Phys. Solids*, 2002, **50**, 2355–2377.
4 W. T. S. Huck, *Nat. Mater.*, 2005, **4**, 271–272.
5 E. P. Chan and A. J. Crosby, *Soft Matter*, 2006, **2**, 324–328.
6 D. Y. Khang, H. Q. Jiang, Y. Huang and J. A. Rogers, *Science*, 2006, **311**, 208–212.
7 J. Genzer and J. Groenewold, *Soft Matter*, 2006, **2**, 310–323.
8 N. Bowden, S. Brittain, A. G. Evans, J. W. Hutchinson and G. M. Whitesides, *Nature*, 1998, **393**, 146–149.
9 X. Jiang, S. Takayama, X. Qian, E. Ostuni, H. Wu, N. Bowden, P. LeDuc, D. E. Ingber and G. M. Whitesides, *Langmuir*, 2002, **18**, 3273–3280.
10 E. P. Chan, E. J. Smith, R. C. Hayward and A. J. Crosby, *Adv. Mater.*, 2008, **20**, 711–716.
11 C. Harrison, C. M. Stafford, W. Zhang and A. Karim, *Appl. Phys. Lett.*, 2004, **85**, 4016.
12 S. Chung, J. H. Lee, M.-W. Moon, J. Han and R. D. Kamm, *Adv. Mater.*, 2008, **20**, 3011–3016.
13 H. G. Allen, *Analysis and design of structural sandwich panels*, Pergamon, New York 1969.
14 X. Chen and J. W. Hutchinson, *Scr. Mater.*, 2004, **50**, 797–801.
15 M.-W. Moon, S. H. Lee, J.-Y. Sun, K. H. Oh, A. Vaziri and J. W. Hutchinson, *Scr. Mater.*, 2007, **57**, 747–750.
16 M.-W. Moon and A. Vaziri, *Scr. Mater.*, 2009, **60**, 44–47.
17 E. Cerda and L. Mahadevan, *Phys. Rev. Lett.*, 2003, **90**, 074302.
18 R. K. Roy and K.-R. Lee, *J. Biomed. Mater. Res., Part B*, 2007, **83b**, 72–84.
19 M. Anil, S. F. Ahmed, J. W. Yi, M.-W. Moon, K.-R. Lee, Y. C. Kim, H. K. Seok and S. H. Han, *Diamond Relat. Mater.*, 2010, **19**, 300–304.
20 M.-W. Moon, J. W. Chung, K.-R. Lee, K. H. Oh, R. Wang and A. G. Evans, *Acta Mater.*, 2002, **50**, 1219–1227.
21 M.-W. Moon, K.-R. Lee, K. H. Oh and J. W. Hutchinson, *Acta Mater.*, 2004, **52**, 3151–3159.
22 Y. Rahmawan, K. J. Jang, M.-W. Moon, K.-R. Lee, K.-S. Kim and K. Y. Suh, *Langmuir*, 2010, **26**, 484–491.
23 M. J. Brett and M. M. Hawkeye, *Science*, 2008, **319**, 1192.
24 J. J. Steele and M. J. Brett, *J. Mater. Sci.: Mater. Electron.*, 2007, **18**, 367–379.
25 K. M. Krause and M. J. Brett, *Adv. Funct. Mater.*, 2008, **18**, 3111–3118.
26 M. T. Taschuk, J. B. Sorge, John J. Steele and M. J. Brett, *IEEE Sens. J.*, 2008, **8**, 1521–1522.
27 M. A. Summers and M. J. Brett, *Nanotechnology*, 2008, **19**, 415203.
28 S. F. Ahmed, J. W. Yi, M.-W. Moon, Y.-J. Jang, B. H. Park, S.-H. Lee and K.-R. Lee, *Plasma Processes Polym.*, 2009, **6**, S860–865.
29 M.-W. Moon, S. H. Lee, J.-Y. Sun, K. H. Oh, A. Vaziri and J. W. Hutchinson, *Proc. Natl. Acad. Sci. U. S. A.*, 2007, **104**, 1130–1133.
30 M.-W. Moon, T.-G. Cha, K.-R. Lee, A. Vaziri and H.-Y. Kim, *Soft Matter*, 2010, DOI: 10.1039/c0sm00126k.
31 A. C. Ferrari and J. Robertson, *Philos. Trans. R. Soc. London, Ser. A*, 2004, **362**, 2477–2512.
32 M. A. Tamor and W. C. Vassell, *J. Appl. Phys.*, 1994, **76**, 3823–3830.
33 R. K. Roy, S. F. Ahmed, J. W. Yi, M.-W. Moon, K.-R. Lee and Y. Jun, *Vacuum*, 2009, **83**, 1179–1183.
34 N. Paik, *Surf. Coat. Technol.*, 2005, **200**, 2170–2174.
35 Y. J. Weng, Y. C. Weng, S.-Y. Yang and L. A. Wang, *Polym. Adv. Technol.*, 2007, **18**, 876–882.
36 D. K. Cai, A. Neyer, R. Kuckuk and H. M. Heise, *Opt. Mater.*, 2008, **30**, 1157–1161.
37 T. K. Shih, C. F. Chen, J. R. Ho and F. T. Chuang, *Microelectron. Eng.*, 2006, **83**, 2499–2503.
38 N. Bowden, W. T. S. Huck, K. E. Paul and G. M. Whitesides, *Appl. Phys. Lett.*, 1999, **75**, 2557.
39 J. Tauc, R. Grigorovic and A. Vancu, *Phys. Status Solidi B*, 1966, **15**, 627–637.
40 B. Pejova and A. Tanusevski, *J. Phys. Chem. C*, 2008, **112**, 3525–3537.
41 S. F. Ahmed, M.-W. Moon and K.-R. Lee, *Thin Solid Films*, 2009, **517**, 4035–4038.
42 P. K. Ghosh, S. F. Ahmed, S. Jana and K. K. Chattopadhyay, *Opt. Mater.*, 2007, **29**, 1584–1590.
43 U. N. Maiti, P. K. Ghosh, S. F. Ahmed, M. K. Mitra and K. K. Chattopadhyay, *J. Sol-Gel Sci. Technol.*, 2007, **41**, 87–92.
44 X. M. He, S. T. Lee, I. Bello, A. C. Cheung and C. S. Lee, *J. Mater. Res.*, 1999, **14**, 1055–1061.
45 S. Ilican, M. Caglar and Y. Caglar, *Appl. Surf. Sci.*, 2010, **256**, 7204–7210.
46 Y. Mei, S. Kiravittaya, M. Benyoucef, D. J. Thurmer, T. Zander, C. Deneke, F. Cavallo, A. Rastelli and O. G. Schmidt, *Nano Lett.*, 2007, **7**, 1676–1679.

